LASER LIGHT-SCATTERING STUDIES OF BULL SPERMATOZOA

I. ORIENTATIONAL EFFECTS

J. D. HARVEY, *Department of Physics, University of Auckland, Auckland, New Zealand*
M. W. WOOLFORD, *Ruakura Agricultural Research Centre, Hamilton, New Zealand*

ABSTRACT Calculations based on the known dimensions of bull spermatozoa show that the scattered light intensity is strongly dependent upon the relative orientation of the particle to the incident beam. The magnitude of this effect is apparently much greater than for other systems where motility has been investigated by dynamic light scattering. The calculations show that the scattering source can be approximated by a small spinning mirror, and consequently the greatest light intensity at the detector results from cells swimming in a direction perpendicular to the scattering vector. The calculations are in substantial agreement with photographic observations, as well as direct measurements of the scattered intensity. Previous treatments of dynamic light scattering from swimming bull spermatozoa based on point scattering models are shown to be incorrect.

INTRODUCTION

Laser light scattering has been used for some years now to study the motility of small swimming organisms. The earliest work on spermatozoa (Bergé et al, 1967) showed that the homodyne spectrum, for light scattered from fish and rabbit sperm, was strongly influenced by the motility of the sample, indicating the value of laser light scattering as an assay of motility. Subsequent work has dealt with a variety of sperm species and analysis techniques (Adam et al., 1969; Dubois et al., 1975; Cooke et al., 1976; Shimizu and Matsumoto, 1976; and Hallett et al., 1978). These studies have largely been concerned with attempts to characterize the swimming speed distribution from autocorrelation of the scattered light intensity.

Generally it has been assumed that spermatozoa behave as point particles moving with constant velocity. This type of analysis is reasonable for motile bacteria, but even in this size range (1–2 μm long) the internal degrees of freedom (wiggling, etc.) can affect the spectrum of the scattered light (Stock and Carlson, 1975; Boon et al., 1974).

Spermatozoa are an order of magnitude larger than bacteria, and in the case of bull or ram sperm, far from spherical. Under these conditions the assumption of point scatterers must be closely examined. Experimental observations of other large-sized flagellates, *Euglena gracillis* (Ascoli et al., 1978), have also pointed to the inadequacy of the point scatterer model.

We have collected correlation data on light scattered from motile bovine spermatozoa for some years now, and have found that the interpretation of the correlation functions requires a

scattering model which takes account of the size, shape, and unusual swimming behaviors of these cells. In this paper the implications of the size and shape of spermatozoan cells for light-scattering experiments are investigated with the use of approximate techniques for the calculation of the scattering amplitude. While these techniques may prove inadequate in their detailed predictions, the general features of the angular distribution of the scattered light are not limited by the approximations. It is found that the cells exhibit a very strong orientational effect, such that the scattered intensity is dominated by the light from those cells swimming in a narrow range of angles which are almost perpendicular to the scattering vector.

THEORY

The simplest way to treat the light scattered from a particle that is large compared with the wavelength of light is to use the Rayleigh-Gans approximation. While this approach may not be adequate to describe accurately the amplitude of the light scattered from a spermatozoa cell in view of its large dimensions, it can be expected that the general features of the scattered amplitude will be apparent from such a treatment. For any scattering particle, the far field amplitude of the scattered electric field from the ith particle may be written

$$A_i(\underset{\sim}{k}) = A_i^0 P_i(\underset{\sim}{k}), \tag{1}$$

where A_i^0 is the Rayleigh limit for small-angle scattering and $P_i(k)$ is a form facter which takes into account the spatial extent of the particle. The Rayleigh-Gans approximation yields $P_i(k)$ in the form

$$P_i(\underset{\sim}{k}) = (1/V_i) \int_{V_i} e^{i\underset{\sim}{k}\cdot\underset{\sim}{r}}\, dV. \tag{2}$$

In this approximation the integration over the volume of the particle assumes that all regions of the particle scatter equally and that the incident plane wave is unaffected by the presence of the scattering particles (i.e., it assumes negligible attenuation of the incident beam). Wyatt (1970) found, for example, that scattering from bacteria (*S. aureus*) was well described by the Rayleigh-Gans theory. Light scattered from spermatozoa is quite exceptional in its angular distribution because of the shape of the primary scattering center (the nucleic-acid-containing head). Bull spermatozoa and several other types of mammalian spermatozoa have a flat leaf-shaped head, and a long thin flagellum. We have found that the scattering pattern can be understood as deriving mainly from scattering from the head of the cell, which has a much greater volume than the flagellum. The major dimensions of the head are well defined (8 μm $\times$ 4.5 μm) and the shape is quite satisfactorily represented by a flat ellipse. The thickness of the head has been variously estimated as 0.7–1.0 μm and in the calculations reported here two models have been used. The head has been represented as either an elliptical slab (semiaxes a and b) of constant thickness (c) or an ellipsoid (of semiaxes a, b, and c).

In the case of the elliptical slab model, the integration over the volume of the particle has been performed numerically by integrating over an elliptical plane section and then summing the amplitudes from separate sections to model the particle as a multielement sandwich. If the head of the cell is modeled as an ellipsoid, the Rayleigh-Gans amplitude can be obtained

analytically. The integral in Eq. 2 can be written as

$$P_i(k) = (1/V)\int_{-r}^{r} e^{ikp} A(p)\, dp, \tag{3}$$

where r is the perpendicular distance from the center of the ellipsoid to a tangent plane normal to $\hat{k}$, p is the perpendicular distance of an arbitrary plane normal to $\hat{k}$ which cuts the ellipsoid with an elliptical cross section of area $A(p)$. A geometrical investigation shows that the area of the ellipse formed by the intersection of the plane $lx + my + nz = p$ with the ellipsoid $x^2/a^2 + y^2/b^2 + z^2/c^2 = 1$ is given by

$$A(p) = (\pi abc/r^3)(r^2 - p^2), \tag{4}$$

where $r = (a^2l^2 + b^2m^2 + c^2n^2)^{1/2}$. From Eqs. 3 and 4, the Rayleigh-Gans amplitude may be written

$$\begin{aligned} P_i(k) &= 3\,[\sin(kr) - kr\cos(kr)]/(kr)^3 \\ &= [9\pi/2(kr)^3]^{1/2} J_{3/2}(kr) \end{aligned} \tag{5}$$

which is the same as that for a sphere of radius r. This result was first obtained for ellipsoids of revolution by Guinier (1939).

For scattering from particles which are very large compared with the wavelength, a quite different approach to calculating the scattering amplitude can be used. The incident wavefront can be divided into a set of rays incident on the particle, each ray being partially reflected and transmitted at the surface of the particle. The resultant scattering pattern is calculated by summing the amplitudes of rays passing through and reflected from the particle, and the amplitude for diffraction around the particle (e.g., Van De Hulst, 1958). In the case of a parallel-sided slab, it can be seen that this approach will lead to a scattered intensity which is dominated by the reflection from the surfaces of the head at most scattering angles, since rays passing through the slab are undeviated and diffraction is concentrated in the forward angle region. Under these circumstances, the scattering can be very usefully approximated by that from a mirror (whose reflectivity may vary with scattering angle due to interference between reflections from both surfaces). The same computational strategy employed to evaluate the Rayleigh-Gans amplitude yields the amplitude from a mirror by using a single element elliptical slab and evaluating the amplitude only for orientations of the head, such that the illuminated side of the head is visible to the detector.

Scattering Calculations

The results of a series of numerical calculations on the scattered intensity as a function of the orientation of a swimming spermatozoan are shown in Fig. 2. The intensity plotted in this figure has been averaged over a rotation of 2π about the long axis of the head, since the cell rotates about this axis as it swims. The averaging was performed by numerical integration of the scattered intensity as a function of head rotation, obtained by repeated evaluation of Eq. 2 either by numerical integration for the elliptical slab model or by use of Eq. 5 for the ellipsoidal model.

The swimming velocity vectors have all been taken to lie in a plane normal to the incident

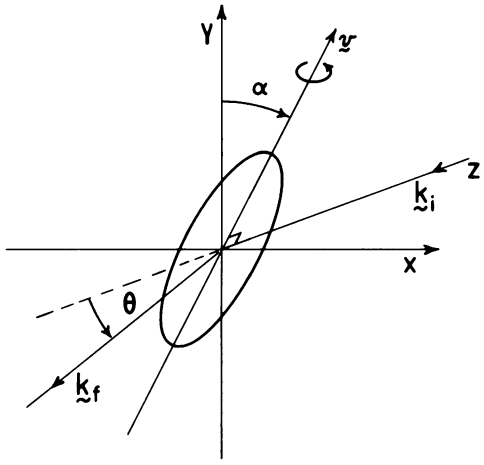

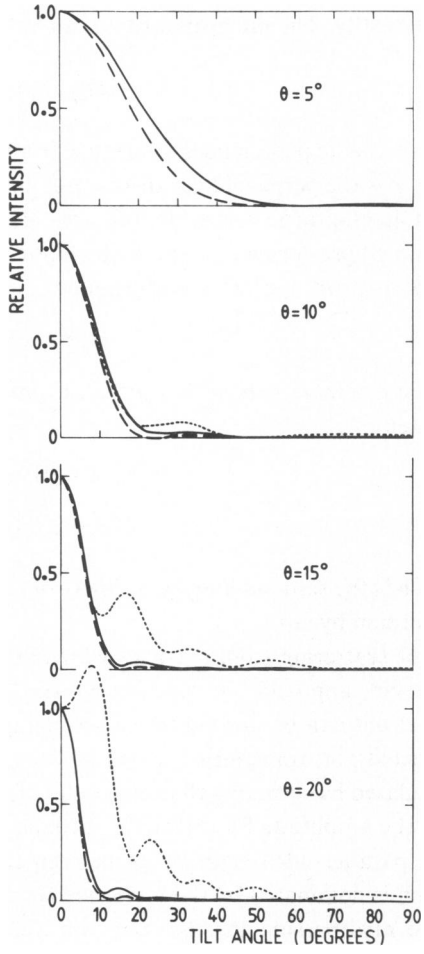

FIGURE 1

FIGURE 2

FIGURE 1 Coordinate system used to model the light from a swimming ellipsoidal spermatozoa. The cell is assumed to rotate about its direction of motion ($\underset{\sim}{v}$). The average intensity is calculated as a function of tilt-angle (α) for various scattering angles.

FIGURE 2 Average scattered intensity at various scattering angles (θ) as a function of tilt-angle (α in Fig. 1) for various theoretical models. Ellipsoid of semiaxes 4.0, 2.25, and 0.5 μm (—). Ellipsoid of semiaxes 4.0, 2.25, and 1.0 μm (---). Spinning opaque elliptical mirror of semiaxes 4.0 and 2.25 μm (— —). The two ellipsoidal models are indistinguishable at $\theta = 5°$. Calculations using a multiple sandwich elliptical slab model of thickness 1.0 μm give results almost indistinguishable from the solid line.

beam, and the scattered intensities are plotted as a function of the tilt-angle defined in Fig. 1. Our observations indicate that motile sperm show a strong tendency to swim on the internal surfaces of the scattering chamber. This is why our analysis deals only with velocities in a plane whose normal is parallel to the incident beam. This marked wall swimming phenomenon has been noted previously (Rothschild, 1963) and more recently analyzed in hydrodynamic terms by Katz and Blake (1975). Its implications for dynamic light-scattering calculations will be considered further elsewhere.

From Fig. 2 it can be seen that the scattered intensity is strongly peaked in the plane whose normal lies along the translation vector. This is true for both elliptical slabs and ellipsoidal shaped heads at forward scattering angles. The differences between the Rayleigh-Gans amplitudes become apparent only at scattering angles such that destructive interference can arise from light scattered from opposite sides of the head. For a head thickness of <1 μm and scattering angles typically employed in dynamic light-scattering studies ($\sim 10°$), the scattering amplitude is essentially the same function of tilt-angle for ellipsoidal and elliptical slab models. Under these circumstances the curve is very close to that given by an opaque spinning mirror of elliptical shape, (i.e., to the amplitude given by the large particle approach discussed earlier, when the scattering is obtained by adding the contributions from different rays reflected and refracted by the cell). The origin of the peaking in the intensity distribution as a function of tilt-angle lies in the strong peak in the curve of intensity versus head rotation angle which arises for specular reflection from the head at a tilt-angle near zero. Detailed investigation shows that the average intensity is dominated by the strength of this "reflective peak," and the average intensity is thus substantially increased for those cells which are swimming in a direction perpendicular to the scattering vector. Eq. 5 permits a simple geometrical interpretation of this effect, since $P_i(k)$ is a maximum when (kr) tends to zero. This maximum value, attained when all scattering elements scatter in phase, occurs either when k tends to zero or when the two tangent planes perpendicular to k become very closely spaced (i.e., when r tends to zero). The minimum value of r is the shortest semiaxis of the ellipsoid and is attained only for vertical orientation of the cell.

As the scattering angle decreases, the intensity versus tilt-angle relationship becomes less sharply peaked; furthermore, all models give similar results, since the thickness of the head is too small to give significant phase differences between rays scattered from opposite sides of the head. It is often asserted that orientational effects can be ignored by performing experiments at a sufficiently small scattering angle, since the form factor $P_i(k)$ tends to unity as θ_{scat} tends to zero. In the case of bull spermatozoa, however, the scattering angles where orientational effects become negligible are experimentally inaccessible. Our calculations show that even at 1° scattering angle the angular distribution of scattered intensity varies significantly with tilt-angle, and that scattering angles below 1° lead to correlation functions which take unreasonable lengths of time to collect and demand extremely high levels of hydrodynamic stability in the suspending medium.

The calculations are sensitive to the detailed geometry of the head (which has not been closely defined) in relation to wavelength and scattering angle, and the secondary peaks in the intensity distributions shown in Fig. 2 should not be accorded any great significance at this stage. In general, the calculations show that because of their small thickness and flat shape, spermatozoan heads can be modeled as rotating mirrors and that a maximum scattered intensity will occur only for cells swimming in such a direction that the normal to the flat surfaces of the head lies close to the direction of the scattering vector at some point during each rotation. Such cells, however, (with $\underset{\sim}{v}$ nearly perpendicular to $\underset{\sim}{k}$) are traveling in such a direction that they impress little or no Doppler shift on the scattered light.

The "spinning mirror" model predicts that the autocorrelation function should exhibit an oscillatory feature with a period corresponding to twice the head rotation rate, since the swimming cells will "flash" when observed by scattered laser light. Weak periodicities on the

appropriate time scale have frequently been observed in the autocorrelation functions we have obtained. These oscillatory features are strongly damped, as would be expected where a spread in velocities (and hence a spread in rotation rates) exists, and generally correspond to a mean rotation rate close to that reported by Gray (1958), who measured the frequency of waves on the flagellum at 9.1 ± 2.9 Hz, and noted that the head rotation was synchronous with these waves.

Photographic Observations

Replacing the photodetector generally used in laser light-scattering studies of sperm motility, with a low power (×30) microscope similarly aligned, provides a dramatic verification of the orientational effect discussed above. The scattering cell used in these experiments was of 1-mm path length having walls oriented normally to the incident beam. After sample insertion, migration of motile cells to the internal surfaces of the cell occurred rapidly (in a time comparable to that required for temperature equilibration). All measurements were performed at a sample temperature of 37°C.

For a scattering vector in the horizontal plane, the majority of sperm cells are observed to swim along trajectories having tilt-angles within ±20% of the vertical for scattering angles in the range 10–30°, with velocities being both upwards and downwards. So marked is the effect that it could easily be mistaken for geotaxis. However, alignment of the scattering vector (and hence the microscope) in the vertical plane results in the cells appearing to swim within a small angle of the horizontal.

These effects are apparent in Fig. 3, which shows a typical microphotograph time exposure (20 s) for swimming bull spermatozoa illuminated with a 628-nm He-Ne laser and observed at a scattering angle of 18.8°. Swimming trajectories appear on the film as a string of dots (a consequence of the flashing effect) and 80% of trajectories fall in the range of tilt-angles $0° < \theta < 20°$.

The range of tilt-angles actually observed can be investigated by counting those tracks on the film which can be distinguished without ambiguity and classifying them according to their angle from the vertical direction. A histogram constructed from the analysis of 171 such tracks on a set of photographs (of which Fig. 3 is one member) is shown in Fig. 4. A detailed agreement between theory and the experimental histogram should not be expected, since the histogram does not measure exactly the average scattered intensity as a function of angle; furthermore, any wobbling or helical motion of the head which causes the long axis to deviate from the translation vector will cause the range of track angles observed to be broadened from that expected for pure spinning motion about this long axis. It is known that spermatozoa swim in approximately helical trajectories, but we have found that the deviation from linear motion, while pronounced at lower temperatures, is not great at 37°C.

Further evidence of the orientational phenomenon may be obtained by viewing immotile cells whose heads become adhered to the cell window. It is usually possible by manipulating the suspending medium in the cell to rotate the spermatozoan about its attachment point by ±90°. The variation so observed in scattered intensity is such that the image formed by the scattered light becomes invisible for tilt-angles >20°.

Examination of the tracks in the photograph of Fig. 3 shows that they all lie in the same focal plane, which was observed to have a depth of field of the order of a few tenths of a

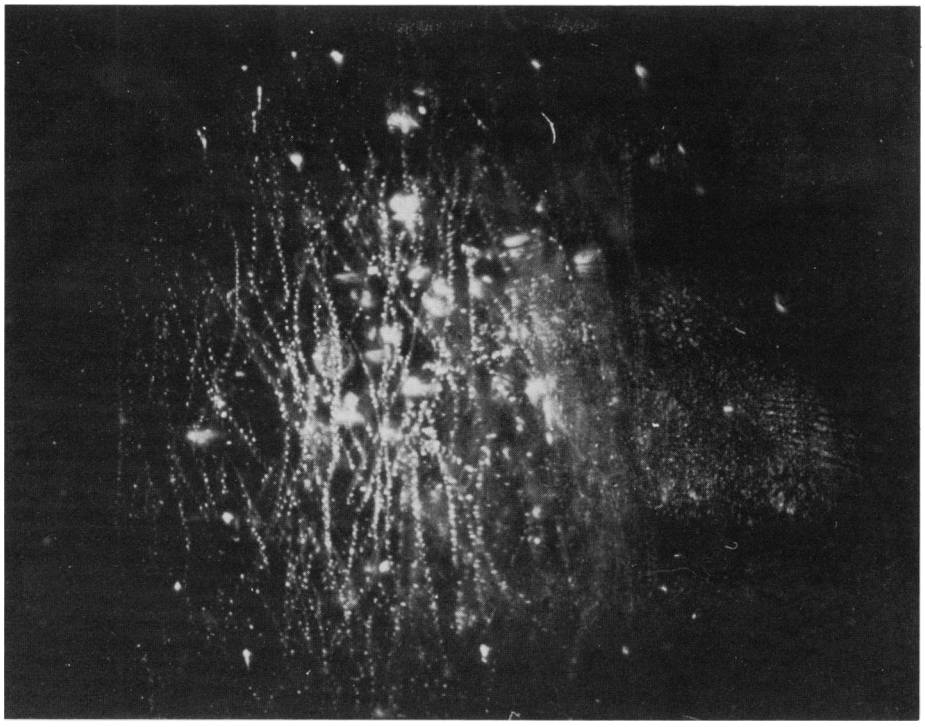

FIGURE 3 Microphotograph time exposure (20 s) of the scattering volume at a scattering angle of 19°, illuminated with a low power He-Ne laser. Swimming trajectories of bull spermatozoa appear as a line of dots. The microscope used was focused on the internal surface of the scattering cells, and the overexposed "flares" on the film were observed to be generated by immotile sperm.

millimeter. This demonstrates the previously mentioned tendency for motile cells to swim on the internal surfaces of the cell (i.e., in the plane normal to the incident beam).

Time Dependence of the Mean Scattered Intensity

Immotile sperm cells sediment at a slow but detectable rate under the influence of gravity. The density of the head is so much greater than that of the flagellum that immotile cells in equilibrium are distributed about a small range of tilt-angles close to 0°. The rate of relaxation back to the equilibrium position has been estimated as $\sim(0.03)\ \sin\phi$ rad s^{-1} (Roberts, 1970), where ϕ is the angle between the tail and the vertical. The calculations reported here imply that the mean scattered intensity for immotile cells will be much greater when this is observed with the scattering vector oriented in the horizontal plane than when it is observed with the scattering vector in the vertical plane (tilt-angles close to 90°). The averaging over all angles of the head in this case will be obtained by the statistical distribution of orientations of dead cells.

The experimentally observed intensity for horizontal and vertical scattering vectors as a function of time after insertion of the sample in the scattering cell (when all orientations of dead cells can be expected in view of turbulent mixing of the sample) is shown in Fig. 5. The shape of these curves is as expected, it being necessary to wait for ~10 min for the immotile

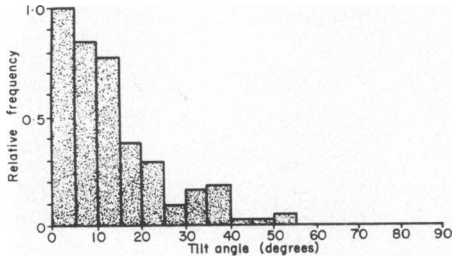

FIGURE 4

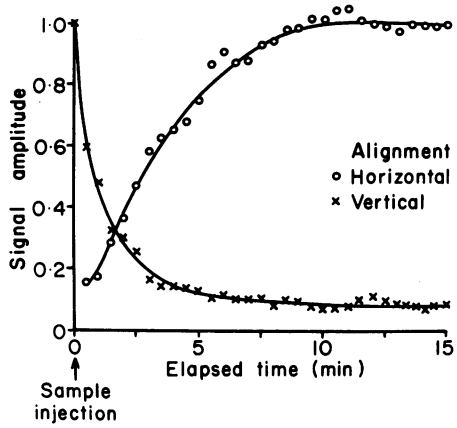

FIGURE 5

FIGURE 4 Histogram of the number of trajectories observed as a function of track angle on a set of photographs similar to Fig. 3. The majority of observed trajectories fall in a narrow range of angles close to the vertical direction for scattering vectors in the horizontal plane.

FIGURE 5 Mean intensity recorded by a detector at a scattering angle of 8° as a function of time after sample insertion with the scattering vector in the horizontal (O) and vertical (X) planes. The change in mean intensity is caused by the relaxation of immotile sperm towards their equilibrium distribution of tilt-angles. After several minutes all immotile sperm are sedimenting with orientations close to the vertical.

cells to reach an equilibrium distribution of orientations. The mean intensity for horizontal alignment is ~80 times greater than that for vertical alignment at a scattering angle of 8°.

DISCUSSION

It has been shown that the intensity of laser light scattered by swimming bull sperm is strongly dependent on the relative orientations of the trajectory and the scattering vector. The intensity distribution as a function of tilt-angle is such that negligible light is scattered to the detector for tilt-angles $\gtrsim 30°$, at the scattering angles generally employed for laser light-scattering experiments.

The phenomenon is most marked where all cells swim in the one plane. This frequently occurs in light-scattering cells as a result of the pronounced tendency for motile spermatozoa to remain swimming close to the internal surfaces. Occasionally, a cell is recorded photographically to be swimming at a large apparent tilt-angle; such cells are inferred to be swimming perpendicular to the scattering vector in the body of the medium.

In dynamic light-scattering (intensity fluctuation spectroscopy) experiments orientational effects will bias the distribution of swimming speeds apparent to the detector and would be expected to significantly increase the autocorrelation decay time. Further serious implications arise from immotile cells, since these rapidly align themselves in a vertical direction (head downwards). Such vertically aligned cells, while visible to a detector aligned at a scattering angle in the horizontal plane, are virtually invisible to a detector aligned at the same scattering angle in the vertical plane. Furthermore, a detector aligned in the horizontal plane will collect

scattered light from almost all immotile cells (as they diffuse rotationally about their long axis) but can receive light from only a small proportion (perhaps 20%) of the motile population. The ratio of the amplitudes of the correlation function components arising from motile and immotile cells cannot thus be expected to yield an absolute estimate of the proportion of live cells unless the orientational effects are fully accounted for.

We conclude, therefore, that neither the swimming speed distribution nor the proportion of motile cells in a sample of bull spermatozoa can be measured by laser light-scattering techniques unless orientational effects are included in the data analysis of the autocorrelation functions. The apparent agreement obtained in some cases between speed distributions derived using a simple point-scattering model at low scattering angles and those obtained by other methods must, therefore, be considered fortuitous.

The calculations reported here can clearly be extended to yield predicted autocorrelation functions. While such an extention may yield useful information on the origin of the fast decaying components of the autocorrelation function of the scattered light, such calculations will depend sensitively upon the precise geometry of the sperm cells, and upon the validity of the Rayleigh-Gans approximation for scattering centers of this size. After submission of this work we learned of the recent paper by Craig et al. (1979) in which it is found by direct numerical computation, using the Reyleigh-Gans approximation and realistic models for the shape and swimming motion of spermatozoa, that the decay of the autocorrelation function of the scattered light is determined predominantly by the rotation rate and not by the translation rate of the cells. This result can be understood readily on the basis of the scattering phenomena described here.

The authors would like to thank Dr. P. Shannon of the New Zealand Dairy Board, Dr. R. Sherlock of the University of Waikato, and Mr. B. Phease of the University of Auckland for helpful discussions during the course of this work.

Received for publication 14 December 1979 and in revised form 1 April 1980.

REFERENCES

ADAM, A., A. HAMELIN, P. BERGÉ, and M. GOFFAUX. 1969. Possibilité d'application de la technique de diffusion inélastique de la lumiere a létude de la vitali té des spermatozoides de taureaux. *Ann. Biol. Anim. Biochim. Biophys.* **9**:657–665.

ASCOLI, C., M. BARBI, C. FREDIANI, and A. MURE. 1978. Measurements of *Euglena* motion parameters by laser light scattering. *Biophys. J.* **24**:585–599.

BERGÉ, P., B. VOLOCHINE, R. BILLARD, and A. HAMELIN. 1967. Mise en évidence du mouvement propre de microorganisms vivants grâce â l'étude de la diffusion inélastique de lumière. *C. R. Acad. Sci. (Paris) Ser. D.* **265**:889–892.

BOON, J. P., R. NOSSAL, and S. O. H. CHEN. 1974. Light scattering due to wiggling motion of bacteria. *Biophys. J.* **14**:847–864.

COOKE, D., F. R. HALLETT, and C. A. V. BARKER. 1976. Motility evaluation of bull spermatozoa by photon correlation spectroscopy. *J. Mechanochem. Cell Motil.* **3**:219–223.

CRAIG, T., F. R. HALLETT, and B. NICKEL 1979. Quasi-elastic light-scattering spectra of swimming spermatozoa. Rotational and translational effects. *Biophys. J.* **28**:457–472.

DUBOIS, M., P. JOUANET, P. BERGÉ, B. VOLOCHINE, C. SERRES, and G. DAVID. 1975. Méthode et apareillage de mesure objective de la mobilite des spermatozoides humains. *Ann. Phys. Biol. Med.* **9**:19–41.

GRAY, J. 1958. The movement of the spermatozoa of the bull. *J. Exp. Biol.* **35**:96–108.

GUINIER, A. 1939. La diffraction des rayons X aux très petits angles: application a l'étude phénomènes ultramicroscopiques. *Ann. Phys. (Paris).* **12**:161–237.

HALLETT, F. R., T. CRAIG, and J. MARSH. 1978. Swimming speed distributions of bull spermatozoa as determined by quasi-elastic light scattering. *Biophys. J.* **21**:203–216.

KATZ, D. F., and J. R. BLAKE. 1975. Flagellar motion near walls. *In* Symposium on Swimming and Flying in Nature. Plenum Press, New York. 173–184.

ROBERTS, A. M. 1970. Motion of spermatozoa in fluid streams. *Nature (Lond.)*. **228**:375–376.

ROTHSCHILD, LORD. 1963. Non random distribution of bull spermatozoa in a drop of sperm suspension. *Nature (Lond.)*. **198**:1221–1222.

SHIMIZU, H., and G. MATSUMOTO. 1976. Photon statistics of laser light scattered by motile spermatozoa. *Opt. Commun.* **16**:197–201.

STOCK, G. B., and F. D. CARLSON. 1975. Photon autocorrelation spectra of wobbling and translating bacteria. *In* Symposium on Swimming and Flying in Nature. Plenum Press, New York. 57–68.

VAN DE HULST, H. C. 1958. Light Scattering by Small Particles. Chapter 8. John Wiley & Sons, Inc., New York.

WYATT, P. J. 1970. Cell wall thickness, size distribution, refractive index ratio and dry weight content of living bacteria. *Nature (Lond.)*. **226**:277–279.